

## INVISCID FLOW FIELD EFFECTS: EXPERIMENTAL RESULTS

L. J. Otten and K. Gilbert

### Introduction

Inviscid effects due to aircraft laser turrets generally manifest themselves as aerodynamic lenses. The resulting optical errors are mainly tilt and focus. Because these effects are approximately steady for a given look angle and Mach number, they would be relatively simple to rectify with adaptive optics systems. It is the purpose of this paper to present the measured tilt and focus for a representative configuration.

### Data Base

The data to be presented include two sources--one theoretical and one empirical. Main flow effects for a sphere were calculated by Wolters (ref. 1) and are presented because a sphere represents a very fundamental laser turret geometry. These estimates are valid for forward-look angles and for Mach numbers less than 0.66. An actual aircraft turret might be a section of a sphere and so would not have as severe a main flow-induced optical effect as a complete sphere. The fact that the sphere will be seen to produce a large effect, however, indicates that inviscid effects must be considered as a credible source of optical degradation.

The experimental data base is derived from the Air Force Weapons Laboratory (AFWL) wind-tunnel tests accomplished on the 0.3 scale Airborne

Laser Laboratory (ALL) Cycle III/IV turret assembly. These experiments were performed in the NASA Ames 14 by 14 foot subsonic tunnel during July/August 1976. The model setup is shown in figure 1. Tunnel Mach numbers ranged from 0.6 to 0.75. The aerodynamic instrumentation that was used to infer steady density consisted of the three linear arrays shown in figure 2. These hemispherical angle of attack pressure probes actually measure local velocity,  $v$ . Local density ( $\rho$ ) then follows from the relationship (ref. 2)

$$\frac{\rho}{\rho_{\infty}} = \left[ 1 - \left( \frac{\gamma - 1}{2} \right) \left( \frac{v^2 - v_{\infty}^2}{a^2} \right) \right]^{(1/(\gamma-1))} \quad (1)$$

where  $\rho_{\infty}$  = free-stream density

$v_{\infty}$  = free-stream velocity

$a$  = speed of sound in gas

$\gamma$  = ration of specific heats

A more complete description of these probes is found in reference 3.

Maximum inviscid effects were observed for  $M = 0.75$ . Data for  $M = 0.75$ ,  $M = 0.60$  and  $M = 0.50$  are shown in figure 3 for three rake locations. The ordinate axis is in units of free-stream density,  $\rho_{\infty}$ . Next, the techniques employed to reduce these data to salient optical parameters are described.

In general, the index of refraction  $n$  and density  $\rho$  are related via the Gladstone-Dale constant  $K$

$$n = 1 + K\rho$$

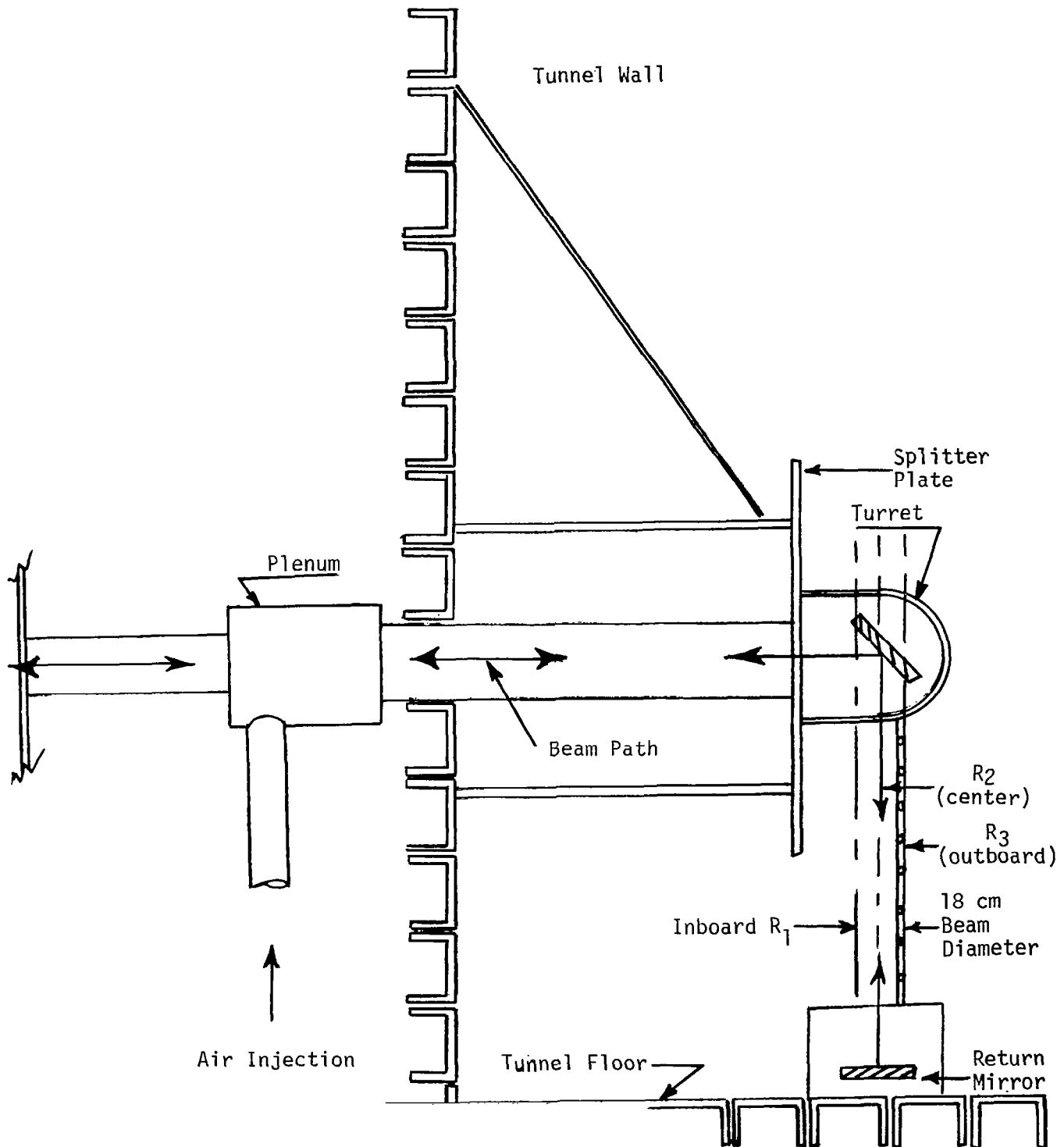


Figure 1. 0.3 Scale All Cycle III/IV APT Cross Section Flow Direction is into Paper ( $R_1$ ,  $R_2$ , and  $R_3$  are steady pressure rakes separated by 9 cm).

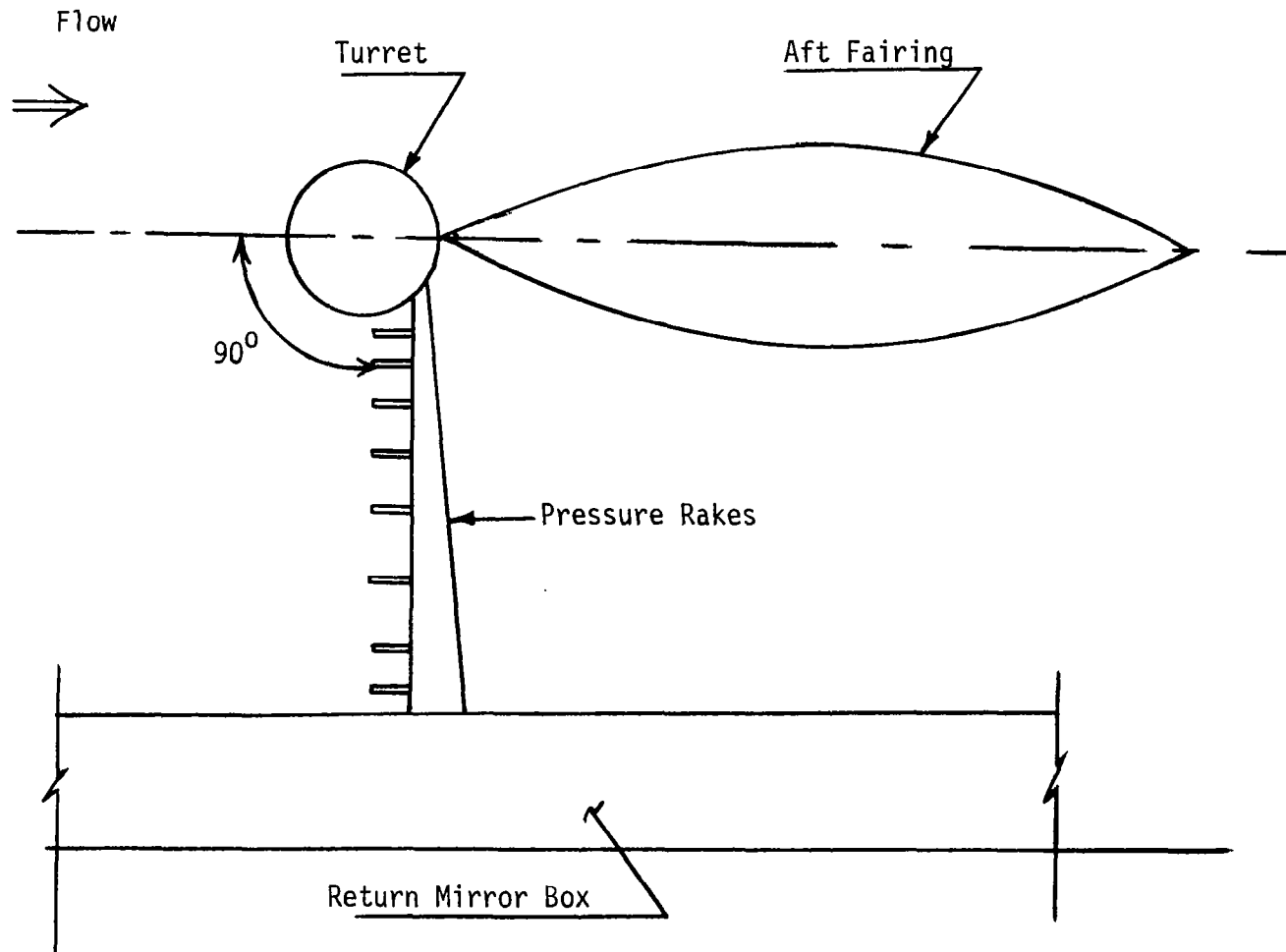


Figure 2. Side View of 0.3 Scale Cycle III/IV APT (Aximuthal angle of rakes is  $90^\circ$ . Elevation angle is  $0^\circ$ , i.e., in plane of flow.)

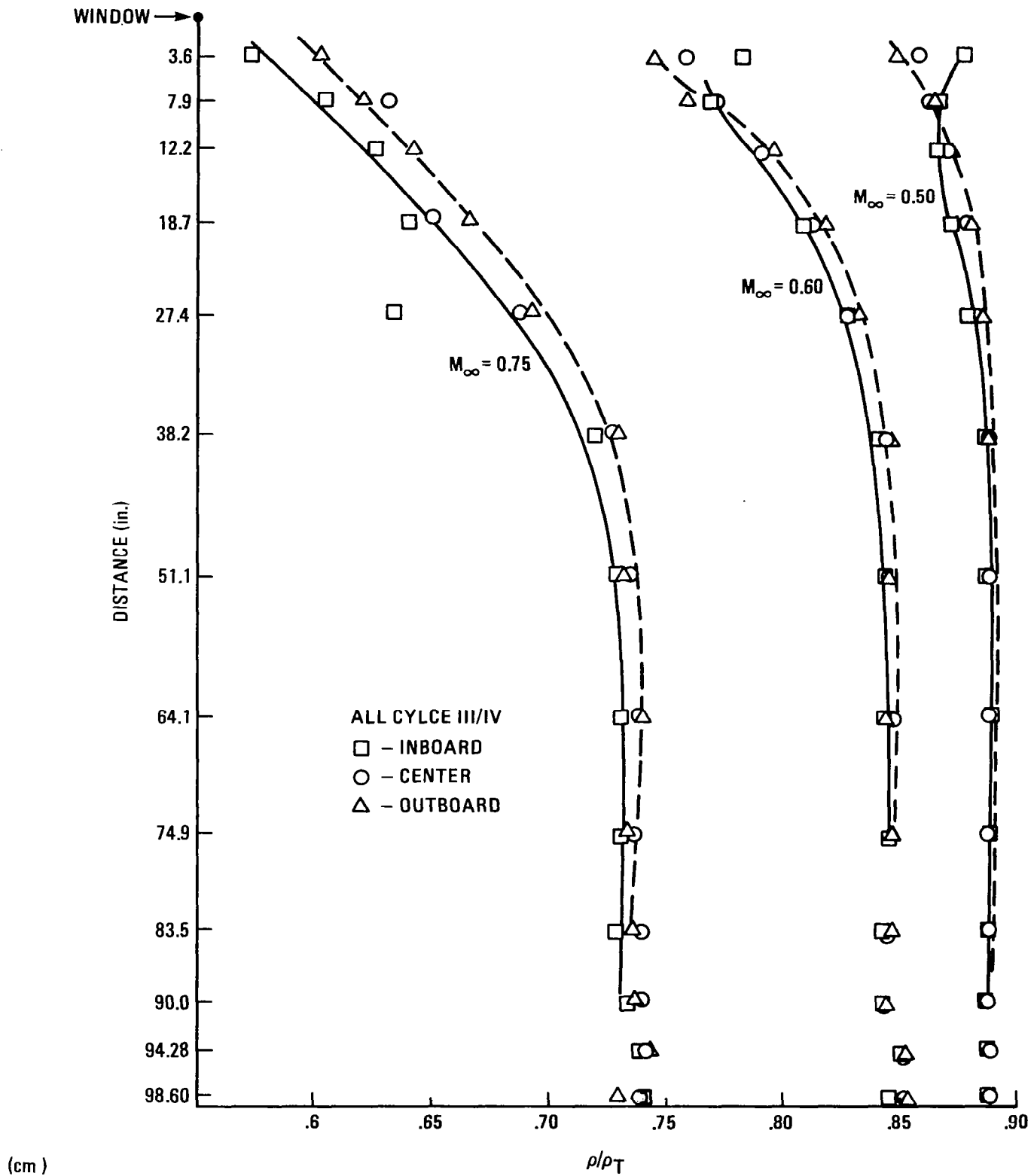


Figure 3. Spatial variation of density.

where  $K = 0.22 \text{ cm}^3/\text{g}$  for laser wavelengths of current interest:

Now the optical phase disturbance  $\Delta\phi$  caused by a density variation across an optical axis is (ref. 4)

$$\Delta\phi = K \int_0^L (\Delta\rho) dz \quad (3)$$

where  $L$  is the propagation distance through the disturbance. Next, the procedure used to estimate  $\Delta\phi$  is detailed:

(a) For each of the three optical paths (figure 1),  $\phi = K \int_0^L \Delta\phi dz$  is calculated, where  $L$  is approximately 75 cm. In addition, a boundary condition is stipulated,  $\Delta\phi(0) = 0$  where the origin is taken as the center of the outgoing wavefront.

(b) The three values of  $\phi$  are then fit with polynomial of form  $\phi = Ax^2 + Bx + C$ . The resulting phase in microns ( $\mu$ ) across the aperture, for a free-stream density of  $1.09 \times 10^{-3} \text{ g/cm}^3$ , is

$$\phi = -3.85x^2 - 2.11x \quad (4)$$

where  $x$  is the distance from the center of the window in units of dimensionless diameter. This function is graphed in figure 4 for  $M = 0.75$ .

(c) Finally, these wind-tunnel measurements included a free-stream density ( $\rho_\infty$ ) of  $1.09 \times 10^{-3} \text{ cm}^3/\text{g}$  and an aperture radius ( $R$ ) of 9 cm. Scaling of results to other altitudes and aperture sizes follows from

$$\phi^1 = \phi \frac{\rho'_\infty}{\rho_\infty} \frac{R^1}{R}$$

Similarly, scaling to other Mach numbers is in accordance with equation (1).

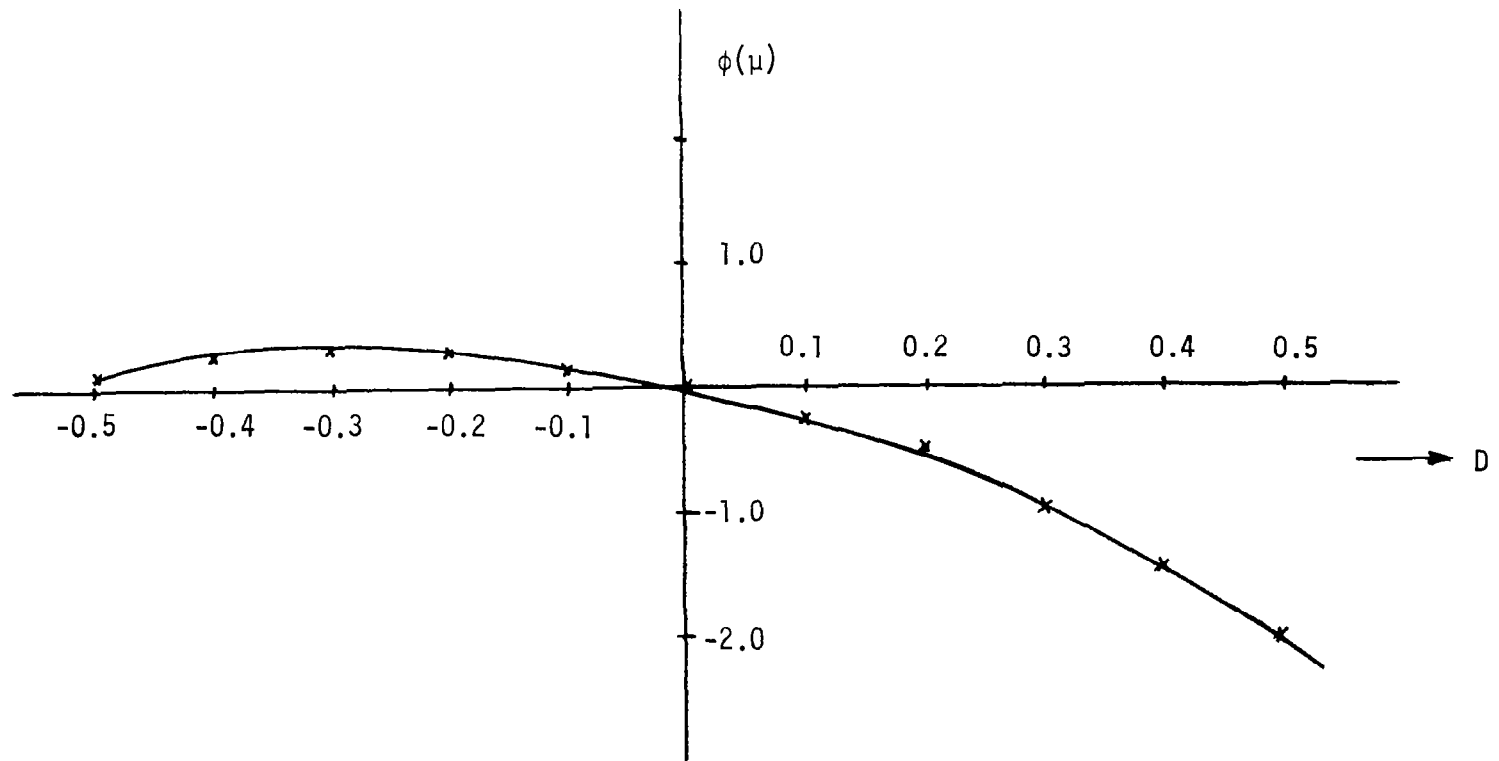


Figure 4. Measured Phase Across Aperture for 0.3 Scale ALL APT Cycle III/IV Turret (The aperture diameter is 18 cm, and the thermal free-stream density is  $\rho_{\infty} = 1.19^{-3} \text{ g/cm}^3$ .)

### Implications of Data

The geometry for the main flow sphere problem is depicted in figure 5, while the results of Wolter's calculation appear in figure 6. A laser turret radius of 25 cm and sea-level atmospheric density are assumed. The wind-tunnel data, scaled to the 25 cm aperture radius, are also shown in figure 6. Notice that the optical path differences calculated from the wind-tunnel data are of the same order as those predicted for the sphere. The fact that these represent markedly different geometries lends credence to the generality of the results.

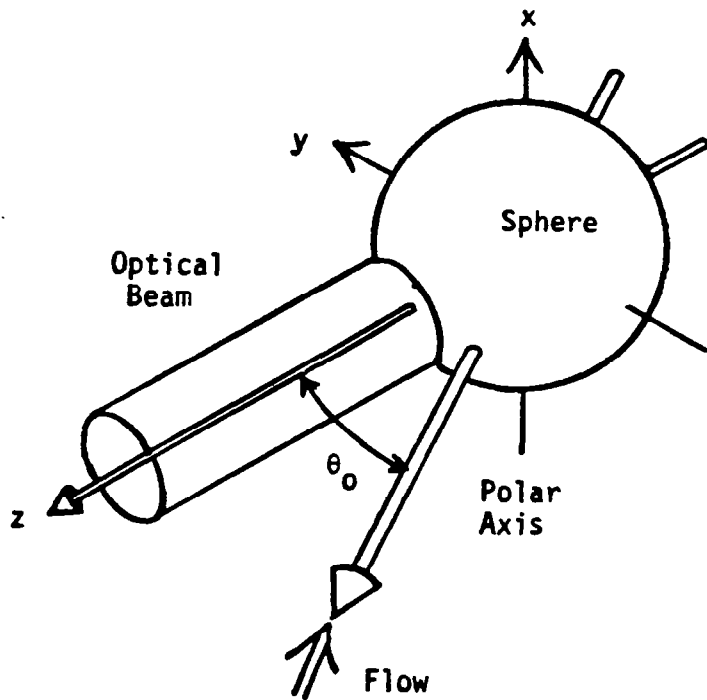
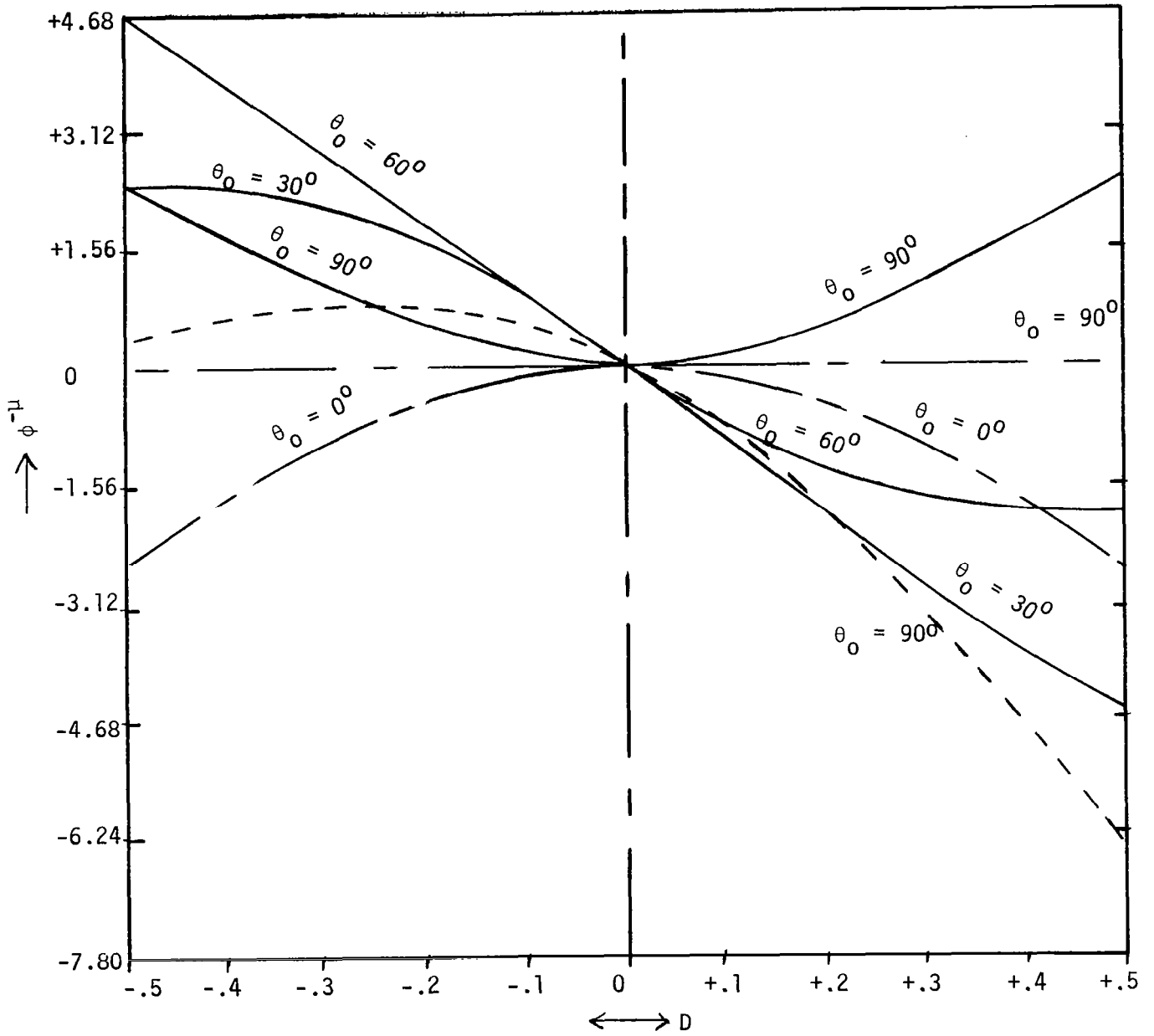


Figure 5. Coordinate System for Main-Flow Sphere Problem.





The solid lines (—) reflect main flow calculations for a sphere at  $M = 0.6$ , while the dashed line (---) represents 0.3 scale ALL turret ( $M = 0.75$ ).  $\theta_0$  is the look angle, while  $\rho_\infty = 1.25^{-3}\text{g/cm}^3$ .

Figure 6. Variation of Optical Path Across 50 cm Diameter Aperture.

The effective focal length of the aero-optical aberration estimated from the 0.3 scale ALL Cycle III/IV fairing can be estimated as follows.

First, equation (4) is rewritten in units of centimeters

$$\phi = -4.93^{-7} x^2 - 1.34^{-5} x \quad (5)$$

with  $0 \leq x \leq 25$  cm

Noting that the coefficient of  $x^2$  is related to the effective focal

length  $F$  by  $\frac{1}{2F} = -4.93^{-7} \text{ cm}^{-1}$  then  $F = -11.1$  km

This represents a fairly weak aerodynamic lens.

### Conclusions

Airborne Laser turrets generally induce invisid flow effects which can lead to laser optical degradations. The magnitude of these aero-optical distortions for future optics system requirements was investigated. Optical path differences across laser turret apertures were estimated from two data sources. The first was a theoretical study of main flow effects for a spherical turret assembly for a Mach number ( $M$ ) of 0.6. The second source was an actual wind-tunnel density field measurement on the 0.3 scale ALL Cycle III/IV laser turret/fairing assembly, with  $M = 0.75$ . A range of azimuthal angles from  $0$  to  $90^\circ$  was considered, while the elevation angle was always  $0^\circ$  (i.e., in the plane of the flow). The calculated optical path differences for these two markedly different geometries were of the same order. Scaling of results to sea level conditions and an aperture diameter of 50 cm indicated up to  $7 \times 10^{-4}$  cm of phase variation across the aperture for certain forward look angles and a focal length of  $F = -11.1$  km. These values are second order for a  $10.6\mu$  system.

## REFERENCES

1. Aerodynamic Effects on Airborne Optical Systems, D. J. Wolters, McDonnell Douglas Report MDC A2582, 1973.
2. Aerodynamics for Engineering Students, Houghton & Brock, Arnold Ltd, 1970.
3. The Dynamics and Thermodynamics of Compressible Fluid Flow, A. H. Shapiro, The Ronald Press Co., New York, 1953.
4. "Flight Calibration Tests of a Nose-Boom-Mounted Fixed Hemispherical Flow-Direction Sensor," NASA TN-D-7461, 1973.